What is already known about this topic

- Clinical research coordinators, who play a vital role in carrying out quality clinical trials, face various problems related to their broadly defined roles and relatively new specialty.
- Research has been required to identify and measure the sources of the job stress of clinical research coordinators.

What this paper adds

- The 23-item Stressor Scale for Clinical Research Coordinators has acceptable validity and reliability for evaluating the sources of clinical research coordinators' stress.
- The six factors are 'quantitative workload', 'conflict with investigators', 'ambiguity of work', 'conflict with other clinical research coordinators and with supervisors', 'demands from an affiliate other than the hospital', and 'difficulty in caring for trial participants'.

Implications for practice and/or policy

- Our instrument makes it possible to assess the work environment of clinical research coordinators.
- Further studies would be helpful to confirm the cross-cultural utility of the instrument.

Norman (2008), suggesting appropriate content validity. SSCRC has concepts similar to the stressors of NIOSH models (Hurrell & McLaney 1988). However, items and factors in SSCRC are modified to suit the situations of CRCs. For example, Factor1 represents work overload of CRCs and corresponds to the stressor 'quantitative workload' in NIOSH model. Work overload is one of the stressors most strongly related to stress reactions (Hurrell & Murphy 1992, Maslach *et al.* 2001). Factor 3 represents ambiguity of the role and career development of CRCs, which has been found in previous studies (Roberts *et al.* 2006). It corresponds to the stressors 'role ambiguity' and 'job future ambiguity' in NIOSH model. Factor 2 and 4 represent interpersonal conflicts with healthcare professionals in clinical trials. However, items of conflict with clinical nurses were deleted from the preliminary SSCRC in the EFA due to low factor loadings, although this conflict has been found in previous studies of CRCs (Spilsbury *et al.* 2008). It may be because CRCs do not have many opportunities to contact clinical nurses in Japan (Matsumoto *et al.* 2011).

Validity and reliability

As results of EFA, a six-factor solution was considered to be the most suitable. CFA is more powerful than EFA, because CFA is a hypothesis testing approach, allowing testing of the goodness of fit of a model generated from EFA (Streiner & Norman 2008). The results of EFA and CFA indicated that SSCRC has acceptable construct validity. The fact that SSCRC had important correlations with burnout and psychological distress supports the concurrent validity, because psychological stress reactions, such as burnout and psychological distress are caused by severe and prolonged exposure to job stressors (Maslach *et al.* 2001, Ikeda *et al.* 2009). However, additional studies are helpful to test concurrent validity, because stressors also lead to physiological and behavioural reactions in NIOSH model (Hurrell & Murphy 1992). The complete convergent and discriminant validity using multitrait scaling analysis also supports the theoretically based factor structure of the scale (Watt *et al.* 2009).

Table 4 Descriptive statistics, internal consistency (n = 589) and test–retest reliability (n = 405) of the SSCRC.

	No. of items	Average scale score* Mean (SD)	Cronbach's alpha	ICC
Total SSCRC	23	2·6 (0·5)	0·88	0·85
Factor 1: Quantitative workload	4	3·0 (1·0)	0·82	0·84
Factor 2: Conflict with investigators	5	2·5 (0·7)	0·81	0·78
Factor 3: Ambiguity of work	5	2·7 (0·8)	0·77	0·76
Factor 4: Conflict with other CRCs and with supervisors	3	2·4 (1·0)	0·82	0·82
Factor 5: Demands from an affiliate other than the hospital	3	2·3 (0·7)	0·76	0·74
Factor 6: Difficulty in caring for trial participants	3	2·5 (0·7)	0·73	0·65

SD, standard deviation; ICC, intra-class correlation coefficients.
*For total SSCRC, sum of all item scores divided by number of items; for each factor, sum of item scores in the factor divided by number of items in the factor.

Thus, it becomes possible to validly evaluate a wide range of stressors for CRCs.

The reliability of SSCRC is considered to be almost sufficient since most of the factors in SSCRC showed good internal consistency and test–retest reliability. The ICC of Factor 6 of 0·65 was a little less than the recommended value (Fayers & Machin 2000). A possible explanation for the low ICC of Factor 6 is that the degree of difficulty in caring for trial participants could change due to participants handled by CRCs. The reliability of Factor 6 should be re-examined.

Conclusion

The 23-item SSCRC has acceptable content validity, construct validity, concurrent validity, convergent and discriminant validity, internal consistency and test–retest reliability. With SSCRC, practitioners, administrators, and researchers can evaluate job stressors for CRCs. Our instrument is valuable for detecting high-risk CRCs and intervening to alleviate stress.

Funding

This study was funded by a grant from Daido Life Welfare Foundation.

Conflict of interest

No conflict of interest has been declared by the authors.

Author contributions

KM, HF, KK and FN were responsible for the study conception and design. KM, KS and FN performed the data collection. KM and KS performed the data analysis. KM was responsible for the drafting of the manuscript. KS, HF, KK, KK and FN made critical revisions to the paper for important intellectual content. HF and FN provided statistical expertise. KM and FN obtained funding. KK and FN provided administrative, technical or material support. FN supervised the study.

References

Aotani E. & Saito Y. (2008) International considerations. Japan. In *Manual for Clinical Trials Nursing*, 2nd edn (Klimaszewski A.D., Aikin J.L., Bacon M.A., DiStasio S.A., Ehrenberger H.E. & Ford B.A., eds), Oncology Nursing Press, Pittsburgh, PA, pp. 391–401.

Chen M.F., Wang R.H., Cheng C.P., Chin C.C., Stocker J., Tang S.M. & Chen S.W. (2011) Diabetes Empowerment Process Scale: development and psychometric testing of the Chinese version. *Journal of Advanced Nursing* 67(1), 204–214.

Cushway D., Tyler P.A. & Nolan P. (1996) Development of a stress scale for mental health professionals. *British Journal of Clinical Psychology* 35(Pt2), 279–295.

Davis A.M., Hull S.C., Grady C., Wilfond B.S. & Henderson G.E. (2002) The invisible hand in clinical research: the study coordinator's critical role in human subjects protection. *Journal of Law, Medicine & Ethics* 30(3), 411–419.

Eaton T. & Pratt C.M. (1990) A clinic's perspective on screening, recruitment and data collection. *Statistics in Medicine* 9(1–2), 137–143.

Fayers P.M. & Machin D. (2000) *Quality of Life: Assessment, Analysis and Interpretation*. John Wiley and Sons, Chichester.

Fisher J.A. (2006) Co-ordinating 'ethical' clinical trials: the role of research coordinators in the contract research industry. *Sociology of Health & Illness* 28(6), 678–694.

Floyd F.J. & Widaman K.F. (1995) Factor analysis in the development and refinement of clinical assessment instruments. *Psychological Assessment* 7(3), 286–299.

Furukawa T.A., Kessler R.C., Slade T. & Andrews G. (2003) The performance of the K6 and K10 screening scales for psychological distress in the Australian National Survey of Mental Health and Well-Being. *Psychological Medicine* 33(2), 357–362.

Furukawa T.A., Kawakami N., Saitoh M., Ono Y., Nakane Y., Nakamura Y., Tachimori H., Iwata N., Uda H., Nakane H., Watanabe M., Naganuma Y., Hata Y., Kobayashi M., Miyake Y., Takeshima T. & Kikkawa T. (2008) The performance of the Japanese version of the K6 and K10 in the World Mental Health Survey Japan. *International Journal of Methods in Psychiatric Research* 17(3), 152–158.

Granda S.E., Duane C.G., Munz D.C. & Cannon J.C. (2009) A study of factors leading to turnover intentions in clinical research coordinators. *The Monitor* 23(5), 55–60.

Gray-Toft P. & Anderson J.G. (1981) The nursing stress scale: development of an instrument. *Journal of Behavioral Assessment* 3(1), 11–23.

Gwede C.K., Johnsson D.J., Roberts C. & Cantor A.B. (2005) Burnout in clinical research coordinators in the United States. *Oncology Nursing Forum* 32(6), 1123–1130.

Higashiguchi K., Morikawa Y., Miura K., Nishijo M., Tabata M. & Nakagawa H. (1998) The job stressor experienced by hospital nurses: development of the nursing job stressor scale and examination of psychometric properties. *The Japanese Journal of Health Psychology* 11(1), 64–72.

Hill G. & MacArthur J. (2006) Professional issues associated with the role of the research nurse. *Nursing Standard* 20(39), 41–47.

Hoglund A.T., Helgesson G. & Eriksson S. (2010) Ethical dilemmas and ethical competence in the daily work of research nurses. *Health Care Analysis* 18(3), 239–251.

Hurrell J.J. Jr & McLaney M.A. (1988) Exposure to job stress-a new psychometric instrument. *Scandinavian Journal of Work, Environment & Health* 14(Suppl. 1), 27–28.

Hurrell J.J. Jr & Murphy L.R. (1992) Psychological Job Stress. In *Environmental and Occupational Medicine*, 2nd edn (Rom W.N., ed.), Little Brown, Boston, MA, pp. 675–684.

Ikeda T., Nakata A., Takahashi M., Hojou M., Haratani T., Nishikido N. & Kamibeppu K. (2009) Correlates of depressive

symptoms among workers in small- and medium-scale manufacturing enterprises in Japan. *Journal of Occupational Health* **51**(1), 26–37.

Karasek R. (1985) *Job Content Questionnaire and User's Guide*. University of Southern California, Los Angeles, CA.

Kessler R.C., Andrews G., Colpe L.J., Hiripi E., Mroczek D.K., Normand S.L., Walters E.E. & Zaslavsky A.M. (2002) Short screening scales to monitor population prevalences and trends in non-specific psychological distress. *Psychological Medicine* **32**(6), 959–976.

Khader Y.S., Airan D.M. & Al-Faouri I. (2009) Work stress inventory for dental assistants: development and psychometric evaluation. *Journal of Public Health Dentistry* **69**(1), 56–61.

Kitaoka-Higashiguchi K. (2005) Burnout as a developmental process among Japanese nurses: investigation of Leiter's model. *Japanese Journal of Nursing Science* **2**(1), 9–16.

Kitaoka-Higashiguchi K., Nakagawa H., Morikawa H., Ishizaki M., Miura K., Naruse Y., Kido T. & Higashiyama M. (2004) Construct validity of the Maslach Burnout Inventory-General Survey. *Stress and Health* **20**, 255–260.

Leiter M.P. (1991) Coping patterns as predictors of burnout: the function of control and escapist coping. *Journal of Organizational Behaviour* **12**, 123–144.

Marine A., Ruotsalainen J., Serra C. & Verbeek J. (2006) Preventing occupational stress in healthcare workers. *Cochrane Database of Systematic Reviews* **18**(4), CD002892.

Maslach C., Jackson S.E. & Leiter M.P. (1996) *Maslach Burnout Inventory Manual*, 3rd edn. Consulting Psychologists Press, Palo Alto, CA.

Maslach C., Schaufeli W.B. & Leiter M.P. (2001) Job burnout. *Annual Review of Psychology* **52**, 397–422.

Matsumoto K., Nagamura F., Ogami Y., Yamashita N. & Kamibeppu K. (2011) Difficulties of nursing staff involved in phase 1 oncology trials in Japan. *Cancer Nursing* **34**(5), 369–375.

Michie S. & Williams S. (2003) Reducing work related psychological ill health and sickness absence: a systematic literature review. *Occupational and Environmental Medicine* **60**(1), 3–9.

Ministry of Health & Labor and Welfare (2007) *MHLW's Initiative for Clinical Trial Promotion Including Standardized IT*. Retrieved from http://www.mhlw.go.jp/topics/bukyoku/isei/chiken/english/01.html on 28 September 2010.

Mueller M.R. & Mamo L. (2002) The nurse clinical trial coordinator: benefits and drawbacks of the role. *Research and Theory for Nursing Practice* **16**(1), 33–42.

Murohashi H. (2007) Fit indices. In *Covariance Structure Analysis: Amos* (Toyoda H., ed.), Tokyo Tosho Publishing, Tokyo, pp. 235–245.

R Development Core Team (2011) *A Language and Environment For Statistical Computing*. R Foundation for Statistical Computing, Vienna, Austria. Retrieved from http://www.R-project.org/ on 15 March 2011.

Rickard C.M., Roberts B.L., Foote J. & McGrail M.R. (2007) Job satisfaction and importance for intensive care unit research coordinators: results from binational survey. *Journal of Clinical Nursing* **16**(9), 1640–1650.

Roberts B.L., Rickard C.M., Foote J. & McGrail M.R. (2006) The best and worst aspects of the ICU research coordinator role. *Nursing in Critical Care* **11**(3), 128–135.

Rout U.R. (2000) Stress amongst district nurses: a preliminary investigation. *Journal of Clinical Nursing* **9**(2), 303–309.

Sanjo M., Morita T., Miyashita M., Shiozaki M., Sato K., Hirai K., Shima Y. & Uchitomi Y. (2009) Caregiving Consequences Inventory: a measure for evaluating caregiving consequences from the bereaved family member's perspective. *Psycho-oncology* **18**(6), 657–666.

Senol-Durak E., Durak M. & Gencoz T. (2006) Development of work stress scale for correctional officers. *Journal of Occupational Rehabilitation* **16**(1), 157–168.

Spilsbury K., Petherick E., Cullum N., Nelson A., Nixon J. & Mason S. (2008) The role and potential contribution of clinical research nurses to clinical trials. *Journal of Clinical Nursing* **17**(4), 549–557.

Streiner D.L. & Norman G.R. (2008) *Health Measurement Scales: A Practical Guide to their Development and Use*, 4th edn. Oxford University Press, Oxford.

Tanimura C., Morimoto M., Hiramatsu K. & Hagino H. (2011) Difficulties in the daily life of patients with osteoarthritis of the knee: scale development and descriptive study. *Journal of Clinical Nursing* **20**(5–6), 743–753.

The Japan Medical Association (2010) *Massive Network for Clinical Trials (MNCT)*. Retrieved from http://www.jmacct.med.or.jp/english/whatwedo/networks/massive.html on 28 September 2010.

Velicer W. (1976) Determining the number of components from the matrix of partial correlations. *Psychometrika* **41**, 321–327.

Watt T., Bjorner J.B., Groenvold M., Rasmussen A.K., Bonnema S.J., Hegedus L. & Feldt-Rasmussen U. (2009) Establishing construct validity for the thyroid-specific patient reported outcome measure (ThyPRO): an initial examination. *Quality of Life Research* **18**(4), 483–496.

Precise Engineering of siRNA Delivery Vehicles to Tumors Using Polyion Complexes and Gold Nanoparticles

Hyun Jin Kim,[†] Hiroyasu Takemoto,[‡] Yu Yi,[§] Meng Zheng,[⊥] Yoshinori Maeda,[§] Hiroyuki Chaya,[⊥] Kotaro Hayashi,[§] Peng Mi,[‡] Frederico Pittella,[⊥] R. James Christie,[⊥] Kazuko Toh,[⊥] Yu Matsumoto,[⊥] Nobuhiro Nishiyama,[‡] Kanjiro Miyata,[⊥,*] and Kazunori Kataoka[†,§,⊥,∥,*]

[†]Department of Materials Engineering, Graduate School of Engineering, The University of Tokyo, Tokyo 113-8656, Japan, [‡]Polymer Chemistry Division, Chemical Resources Laboratory, Tokyo Institute of Technology, Yokohama 226-8503, Japan, [§]Department of Bioengineering, Graduate School of Engineering, The University of Tokyo, Tokyo 113-8656, Japan, [⊥]Center for Disease Biology and Integrative Medicine, Graduate School of Medicine, The University of Tokyo, Tokyo 113-0033, Japan, and [∥]Center for NanoBio Integration, The University of Tokyo, Tokyo 113-8656, Japan

ABSTRACT For systemic delivery of siRNA to solid tumors, a size-regulated and reversibly stabilized nanoarchitecture was constructed by using a 20 kDa siRNA-loaded unimer polyion complex (uPIC) and 20 nm gold nanoparticle (AuNP). The uPIC was selectively prepared by charge-matched polyionic complexation of a poly(ethylene glycol)-*b*-poly(L-lysine) (PEG-PLL) copolymer bearing ~40 positive charges (and thiol group at the ω-end) with a single siRNA bearing 40 negative charges. The thiol group at the ω-end of PEG-PLL further enabled successful conjugation of the uPICs onto the single AuNP through coordinate bonding, generating a nanoarchitecture (uPIC-AuNP) with a size of 38 nm and a narrow size distribution. In contrast, mixing thiolated PEG-PLLs and AuNPs produced a large aggregate in the absence of siRNA, suggesting the essential role of the preformed uPIC in the formation of nanoarchitecture. The smart uPIC-AuNPs were stable in serum-containing media and more resistant against heparin-induced counter polyanion exchange, compared to uPICs alone. On the other hand, the treatment of uPIC-AuNPs with an intracellular concentration of glutathione substantially compromised their stability and triggered the release of siRNA, demonstrating the reversible stability of these nanoarchitectures relative to thiol exchange and negatively charged AuNP surface. The uPIC-AuNPs efficiently delivered siRNA into cultured cancer cells, facilitating significant sequence-specific gene silencing without cytotoxicity. Systemically administered uPIC-AuNPs showed appreciably longer blood circulation time compared to controls, *i.e.*, bare AuNPs and uPICs, indicating that the conjugation of uPICs onto AuNP was crucial for enhancing blood circulation time. Finally, the uPIC-AuNPs efficiently accumulated in a subcutaneously inoculated luciferase-expressing cervical cancer (HeLa-Luc) model and achieved significant luciferase gene silencing in the tumor tissue. These results demonstrate the strong potential of uPIC-AuNP nanoarchitectures for systemic siRNA delivery to solid tumors.

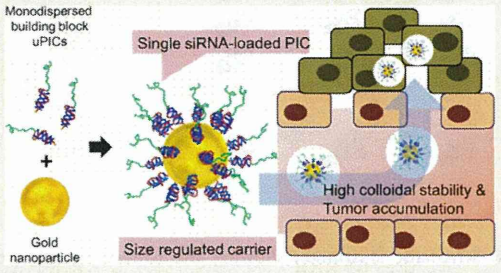

KEYWORDS: siRNA delivery · unimer polyion complex · gold nanoparticle · cancer therapy

Small interfering RNA (siRNA), which induces the sequence-specific degradation of mRNA in the cytoplasm (termed RNA interference (RNAi)), has attracted much attention in cancer therapy.[1,2] However, systemically administered siRNA is rapidly degraded by RNases in the bloodstream and/or eliminated through kidney filtration because they are smaller than 6 nm.[3,4] Thus, siRNA carriers need to be developed in order to overcome these issues for successful therapy. A variety of synthetic nanocarriers have been constructed mainly with cationic nanomaterials, such as lipids, polycations, inorganic nanoparticles, and their hybrid systems.[5−10] These nanocarriers can protect siRNA from enzymatic degradations and apparently increase its size to circumvent kidney filtration. This allows the siRNA payloads to accumulate in tumor tissues through the leaky tumor vasculature *via* the so-called enhanced permeability and retention (EPR) effect.[11,12] In this regard, several recent studies have revealed that precise size-tuning promotes the selective accumulation of nanoparticles in tumor tissues.[13,14] Nanoparticles with a size that is smaller than 50 nm can efficiently

* Address correspondence to kataoka@bmw.t.u-tokyo.ac.jp, miyata@bmw.t.u-tokyo.ac.jp.

Received for review April 17, 2014 and accepted August 18, 2014.

Published online August 18, 2014
10.1021/nn502125h

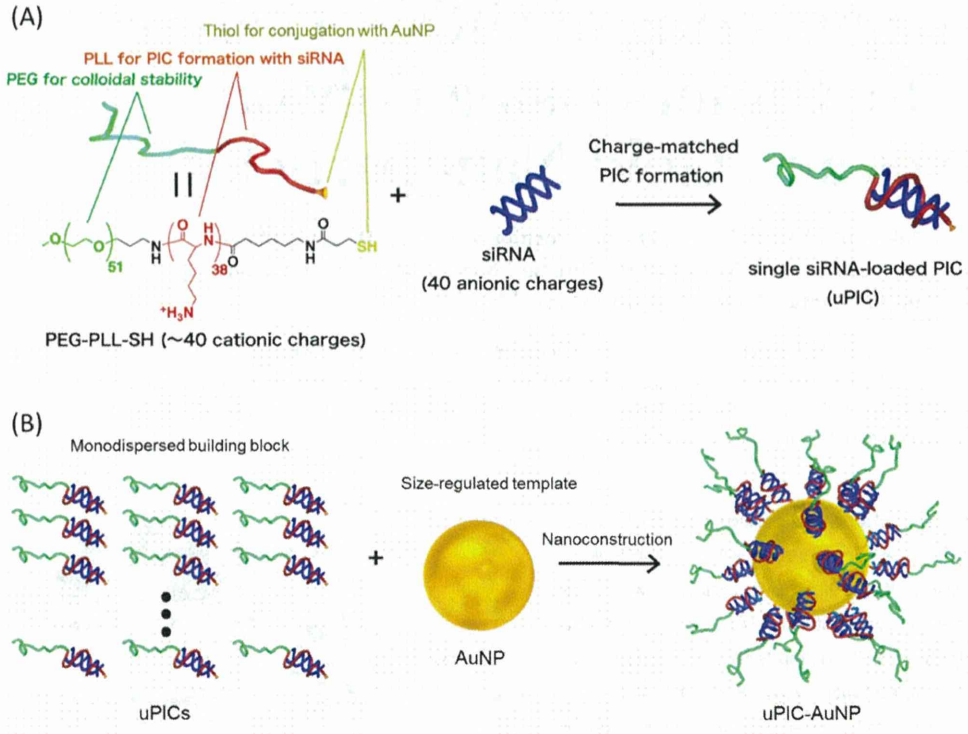

Figure 1. Schematic illustration showing the nanoconstruction of uPIC-AuNPs from monodispersed building blocks. (A) Formation of uPICs comprising a single pair of PEG-PLL and siRNA. (B) Thiol-gold coordination complex between uPICs and AuNP.

accumulate in tumor tissues, especially in a poorly permeable pancreatic tumor model.[13] Thus, the size of nanocarriers is important for enhancing siRNA accumulation in a variety of tumor tissues.

While multimolecular self-assemblies of siRNA with oppositely charged nanomaterials have been widely developed because of their facile and efficient encapsulation of siRNA, it is difficult to control the size and the distribution of these carriers. In contrast, the bottom-up nanocarrier construction with monodispersed building blocks and a nanotemplate enables more precise size-tuning at the nanoscale. With regard to such building blocks, our recent study demonstrated that a block copolymer of poly(ethylene glycol) and poly(L-lysine) (PEG-PLL) with a controlled degree of polymerization of PLL (DP_{PLL}) formed a unimer polyion complex (uPIC)[15] comprising a single siRNA molecule,[16,17] potentially serving as a monodispersed building block. A building-block-loading nanotemplate is necessary to satisfy the Janus-type property requirement for the selective siRNA release into the cytosol. Gold nanoparticles (AuNPs) are promising biocompatible nanotemplates, as their size can be precisely controlled with a narrow distribution, and also they can be coated with polymers or biomolecules through thiol chemistry.[18,19] This type of bonding is relatively stable under extracellular conditions, but these polymers or biomolecules can be competed off the AuNP with glutathione (GSH), which is abundant in the cytosol.[20] Subsequently, the GSH-coordinated anionic AuNPs may interact with uPICs to destabilize them for triggered siRNA release.

To achieve an efficient systemic siRNA delivery to solid tumors, we developed a size-regulated and reversibly stabilized nanoarchitecture (uPIC-AuNP) by utilizing an AuNP template and a monodispersed uPIC building block prepared with a single siRNA/PEG-PLL pair (Figure 1). To this end, a PEG-PLL was prepared to have a DP_{PLL} of ~40 (matched with the negative charges of 21mer/21mer siRNA) and thiol groups at the ω-end of PLL for coordinate bonding with AuNP. After confirming stable binding between single siRNA molecules and copolymers, the resulting uPICs were conjugated to a 20 nm AuNP to build uPIC-AuNP nanoarchitectures exhibiting sizes less than 50 nm and narrow size distributions under biological conditions. The uPIC-AuNPs achieved efficient siRNA accumulation in a subcutaneous tumor model by systemic administration and successfully induced sequence-specific gene silencing in the tumor tissue.

RESULTS AND DISCUSSION

Preparation and Characterizations of uPICs Comprising a Single PEG-PLL/siRNA Pair. PEG-PLL synthesis was targeted to possess 40 positive charges (or DP_{PLL} = 40), as it can complementarily neutralize the negative charges

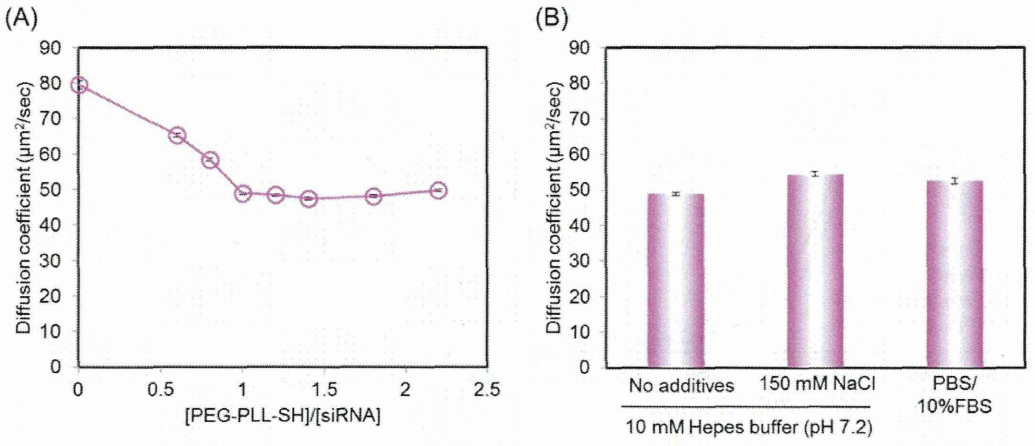

Figure 2. (A) Change in the diffusion coefficient of Cy3-siRNA upon polyionic complexation with PEG-PLL-SH in 10 mM Hepes buffer (pH 7.2) (Cy3-siRNA concentration = 10 nM). Results are expressed as mean and standard deviation (n = 10). (B) Diffusion coefficients of Cy3-siRNA-containing PICs prepared at [PEG-PLL-SH]/[siRNA] = 1.0 in various media (Cy3-siRNA concentration = 10 nM). Results are expressed as mean and standard deviation (n = 10).

of single 21mer/21mer siRNA and form uPICs through charge-matched polyionic complexation (Figure 1). The obtained PEG-PLL with TFA protective groups (PEG-PLL(TFA)) was determined to possess the DP_{PLL} of 38 in ^{1}H NMR spectrum (data not shown). The primary amine in the ω-end of PEG-PLL(TFA) was further modified with LC-SPDP for thiol-gold coordinate bonding, and the quantitative introduction of LC-SPDP was confirmed in ^{1}H NMR spectrum (Figure S1, Supporting Information (SI)). After successive removals of TFA and pyridyl groups with sodium hydroxide and dithiothreitol (DTT), respectively, the thiolated PEG-PLL (PEG-PLL-SH) was mixed with Cy3-labeled siRNA (Cy3-siRNA) at varying mixing ratios in 10 mM Hepes buffer (pH 7.2), and then characterized by fluorescence correlation spectroscopy (FCS). Note that FCS can determine a diffusion coefficient (D) of highly dilute fluorescent molecules even in serum-containing media.[21,22] The D values of PEG-PLL-SH/Cy3-siRNA mixtures decreased progressively with a molar ratio of PEG-PLL-SH to siRNA ([PEG-PLL-SH]/[siRNA]) and leveled off at [PEG-PLL-SH]/[siRNA] = 1 (Figure 2A). The initial decrease in the D indicates PIC formation between Cy3-siRNA and PEG-PLL-SH. The following plateau region in the D strongly suggests that all the Cy3-siRNAs were complexed with PEG-PLL-SH at [PEG-PLL-SH]/[siRNA] = 1, and an excess amount of PEG-PLL-SH at [PEG-PLL-SH]/[siRNA] > 1 did not bind to siRNA. The PIC prepared at [PEG-PLL-SH]/[siRNA] = 1 was further characterized by analytical ultracentrifugation (AUC) based on the absorbance at 260 nm for a precise structural determination. The molecular weight (MW) of PICs in 10 mM Hepes buffer (pH 7.2) containing 150 mM NaCl was calculated by combining the AUC (sedimentation equilibrium) data with a partial specific volume (PSV) of PICs (0.602 cm^3/g) and the buffer density (1.005 cm^3/g). Note that the PSV of PICs was determined as a mass average of PSV of siRNA (0.508 cm^3/g) and PSV of PEG-PLL (0.753 cm^3/g). The major parameters used for the calculation of MW of PICs are summarized in Table S1 (SI). The PIC exhibited a MW of approximately 22 kDa, consistent with the formation of a uPIC comprising a single pair of PEG-PLL (MW = 7200 Da) and siRNA (MW = 13 300 Da). Single siRNA loading in uPIC was confirmed by using FCS. The association number of siRNA in the PIC was determined to be 0.9 ± 0.1 using 10 nM Cy3-siRNA. It was calculated by normalizing the fluorescent particle number (or amplitude number particle) of the PIC to that of naked siRNA. Note that the diffusion coefficient of uPICs determined at 10 nM siRNA (~50 μm^2/sec) was maintained even at much higher concentrations, *i.e.*, 20 and 40 μM siRNA (Table S2 (SI)), indicating that the similar uPICs were also prepared under the preparation condition of uPIC-AuNPs (17 μM siRNA). The uPIC formation with a single pair of siRNA and PEG-PLL (DP of PLL = ~40) can be further validated from the standpoint of their molecular structures. Considering the fact that siRNA adopts a right-handed A-form helix with 11 bp per helical turn, a helical pitch of 2.8 nm, and a diameter of 2.3 nm,[23] PLL segment having the maximum main chain length of 4.1 nm per 11 amino acids and the maximum side chain length of 0.65 nm can completely make ion pairs with siRNA phosphates along the helical structure. Nevertheless, the complete ion pair formation between siRNA and PLL remains to be evidenced in further studies. The stability of uPICs prepared at [PEG-PLL-SH]/[siRNA] = 1 was further investigated by FCS (Figure 2B). The addition of 10% fetal bovine serum (FBS) and a physiological salt hardly affected the D values of the uPICs, indicating stable PIC formation under the biological conditions. These results demonstrated that the stable uPICs were selectively prepared using

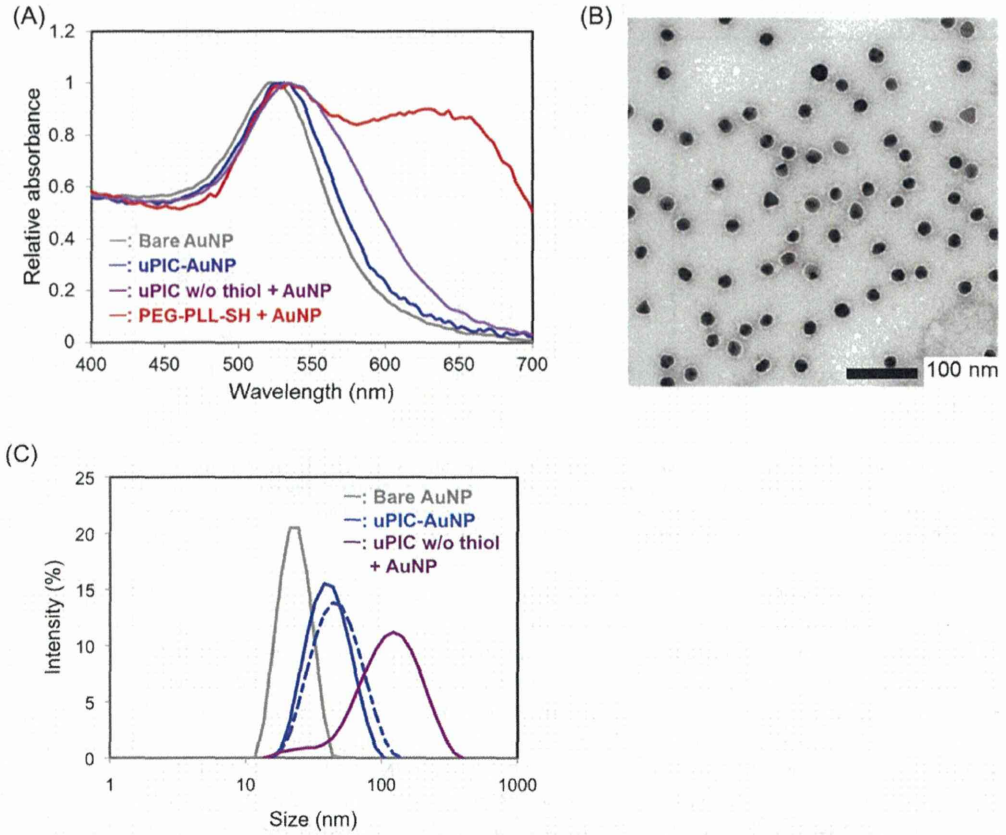

Figure 3. (A) UV−vis absorbance spectra of various sample solutions. Bare AuNP: AuNPs without PICs in 10 mM Hepes buffer (pH 7.2), uPIC-AuNP: uPIC-loaded AuNPs in 10 mM Hepes (pH 7.2) containing 150 mM NaCl, uPIC w/o thiol + AuNP: the mixture of AuNPs and uPICs prepared with nonthiolated PEG-PLL in 10 mM Hepes (pH 7.2) containing 150 mM NaCl, and PEG-PLL-SH + AuNP: the mixture of AuNPs and thiolated PEG-PLL without siRNA. (B) TEM image of uPIC-AuNPs. (C) Intensity-based DLS histograms of various sample solutions. Bare AuNP: AuNPs without PICs in 10 mM Hepes buffer (pH 7.2), uPIC-AuNP: uPIC-loaded AuNPs in 10 mM Hepes (pH 7.2) containing 150 mM NaCl (solid line) or 10% FBS (dashed line), and uPIC w/o thiol + AuNP: the mixture of AuNPs and uPICs prepared with nonthiolated PEG-PLL in 10 mM Hepes (pH 7.2) containing 150 mM NaCl. All samples were incubated overnight at ambient temperature (AuNP concentration: 12 nM).

PEG-PLL bearing ~40 positive charges, allowing their use as monodispersed building blocks for nanoconstruction.

Preparation and Characterizations of the Smart uPIC-AuNP Nanoarchitecture. uPICs were used as monodispersed building blocks for the construction of smart uPIC-AuNP nanoarchitectures (Figure 1). Specifically, the uPICs, which were prepared at [PEG-PLL-SH]/[siRNA] = 1 in 10 mM Hepes buffer (pH 7.2), were mixed with 20 nm AuNPs at a molar ratio ([siRNA]/[AuNP]) = 360 in the same buffer, then incubated at 4 °C for 8 h. Unbound uPICs were removed thoroughly by repeated centrifugal steps and the resulting uPIC-AuNPs were dispersed in 10 mM Hepes buffer (pH 7.2) containing 150 mM NaCl. The successful conjugation of uPICs onto AuNP was verified by UV−vis absorbance spectra, transmission electron microscopy (TEM), and dynamic light scattering (DLS). The absorbance spectrum of uPIC-AuNPs suggested that flocculation of AuNPs hardly occurred during the conjugation process, as a notable change in the absorbance spectra based on the surface plasmon resonance was not observed between bare AuNPs and uPIC-AuNPs (Figure 3A). Furthermore, the TEM image depicted that the uPIC-AuNPs were composed of single AuNP without particle aggregation, as their spherical shapes with a narrow size distribution (Figure 3B) were similar to those of the bare AuNP templates (Figure S2 (SI)). On the other hand, the intensity-based DLS histograms clearly show an increase in size of AuNPs after uPIC conjugation (Figure 3C). The peak top in the histogram was shifted from *ca.* 23 nm in bare AuNPs to *ca.* 38 nm in uPIC-AuNPs. Considering that the siRNA length is *ca.* 6 nm[24] and a hydrodynamic radius of PEG (MW = 2200) in a random coil is *ca.* 1.5 nm,[25] this size increase is consistent with the conjugation of uPICs on AuNP, as illustrated in Figure 1B. In addition, the zeta-potential of uPIC-AuNPs was determined to be −24.7 ± 0.4 mV. This value was significantly higher in the positive direction than that of bare AuNPs (−31.3 ± 1.2 mV), consistent with the presence of PEG outer shell in uPIC-AuNPs. It should be noted that the uPIC-AuNPs maintained their

size and size distribution even after overnight incubation in 10% FBS-containing media (Figure 3C), indicating the high stability of these nanoarchitectures in the biological media. These results clearly demonstrate that the uPIC-AuNPs were successfully constructed in a size-regulated and monodispersed manner.

Next, the number of uPICs (or siRNAs) loaded in the uPIC-AuNPs was determined using a fluorescently labeled siRNA. The uPIC-AuNPs prepared with Alexa647-labeled siRNA (Alexa-siRNA) were treated with an excess amount of mercaptoethanol (12 mM) to induce a thiol exchange reaction on the AuNP surface.[19] The amount of released uPIC was quantified from its fluorescence intensity in the supernatant according to the standard curve (Figure S3 (SI)), and normalized by the amount of AuNP in solution. The number of loaded uPICs was calculated to be *ca.* 20 per AuNP. This value is slightly smaller than that for previous siRNA-loaded AuNP systems, where thiolated siRNAs were directly attached to AuNPs and the number of loaded siRNA amounted to *ca.* 30 per AuNP.[26] The difference between these two formulations could be explained by their different spacer length between thiol and the charged segment. The thiolated siRNA had a longer spacer than the present PEG-PLL-SH polymer, alleviating the steric repulsive effects on the AuNP surface.

With regard to the nanoconstruction of uPIC-AuNPs, it was verified whether the preformation of uPICs and the thiol moiety in PEG-PLL-SH were indispensable for successful preparation of the uPIC-AuNPs. When PEG-PLL-SH polymers were directly mixed with AuNPs prior to PIC formation (or in the absence of siRNA), visible flocculates were formed as indicated by the red-shift in their UV–vis absorbance spectrum (Figure 3A),[18] probably due to consecutive electrostatic binding between negatively charged citrate-stabilized AuNPs and oppositely charged PLL segments. On the other hand, the mixing between AuNPs and uPICs prepared with nonthiolated PEG-PLL led to the formation of considerably larger nanoparticles (DLS peak top: ~120 nm) with a broader size distribution (Figure 3C) and a slightly broader absorbance spectrum (Figure 3A) compared to the uPIC-AuNPs. This result indicates that a large number of AuNPs aggregated into larger particles under the physiological salt condition as a result of low colloidal stability through ineffective surface PEGylation in the absence of thiol-gold coordinate bonding. Note that bare AuNPs immediately aggregated to form visible flocculates by salting-out effect under the same condition (data not shown). Thus, the successful preparation of uPIC-AuNPs may stem from (i) the charge-neutralization of cationic PLL segment with siRNA, which reduces the electrostatic adsorptions between PLL chains and AuNPs, and (ii) the effective conjugation of uPICs (or PEG chains) onto AuNPs through thiol-gold coordinate bonding, which enhances colloidal stability.

The reversible stability of uPIC-AuNPs was verified by mimicking cytoplasmic reductive conditions as well as the extracellular conditions. The nanoarchitectures were incubated in a heparin solution with or without 10 mM GSH, which corresponds to the cytoplasmic concentration. In this stability assay, heparin was used as a representative of glycocalyx that is a major component of extracellular matrices and is abundant in the renal basement membrane. Glycocalyx is considered as a major obstacle for PIC-based siRNA delivery because PICs might be disrupted through electrostatic interactions with the negatively charged matrices.[27] In the absence of heparin and GSH, almost no bands derived from siRNA were observed for both uPICs and uPIC-AuNPs (Figure 4A), confirming the polyionic complexation of siRNA as indicated by the FCS result (Figure 2A). It should be noted that the staining of siRNA with SYBR Green II was significantly impaired when siRNA forms PICs with PEG-PLL, leading to almost no fluorescence signal from the siRNAs loaded by uPICs as well as uPIC-AuNPs. The heparin treatment induced a concentration-dependent siRNA release from uPICs and uPIC-AuNP by counter polyanion exchange. However, this release required more heparin in the case of uPIC-AuNPs compared to uPICs. In particular, while the released siRNA was clearly observed upon treatment of uPICs with 1 μg/mL of heparin, almost no band was detected for uPIC-AuNPs under the same conditions. These results indicate that uPICs conjugated onto the AuNP were more stable than free uPICs. This enhanced PIC stability may be attributed to the PEG outer layer surrounding uPIC-AuNP.

In contrast, the GSH-treated uPIC-AuNPs showed a band of released siRNA with smaller amount of heparin, compared to those in the absence of GSH, demonstrating the GSH-responsive siRNA release from uPIC-AuNPs. The underlying mechanism for this GSH-responsive release can be explained as follows. GSH (or its cystein thiol) can detach uPICs from AuNP through the thiol–thiol exchange reaction. The detached uPICs should become more sensitive for counter polyanion exchange with heparin as indicated by Figure 4A (uPIC + Heparin lanes *vs* uPIC-AuNP + Heparin lanes), resulting in the facilitated siRNA release. This can be explained by the fact that the cysteine thiol in GSH can competitively interact with coordinate bonds between uPICs and AuNP, forming alternative coordinate bonds with AuNPs (or uPICs) that promote the detachment of uPICs from uPIC-AuNPs. In this regard, it is worth mentioning that the GSH-treated uPIC-AuNPs also released siRNA in the absence of heparin. GSH alone did not release siRNA from uPICs even at 50 mM (Figure 4B), suggesting that the coexistence of GSH and AuNPs should be crucial for the siRNA release. We assumed that GSH-conjugated AuNPs (GSH-AuNPs), which should be generated by incubation of uPIC-AuNPs with GSH, might elicit siRNA release from

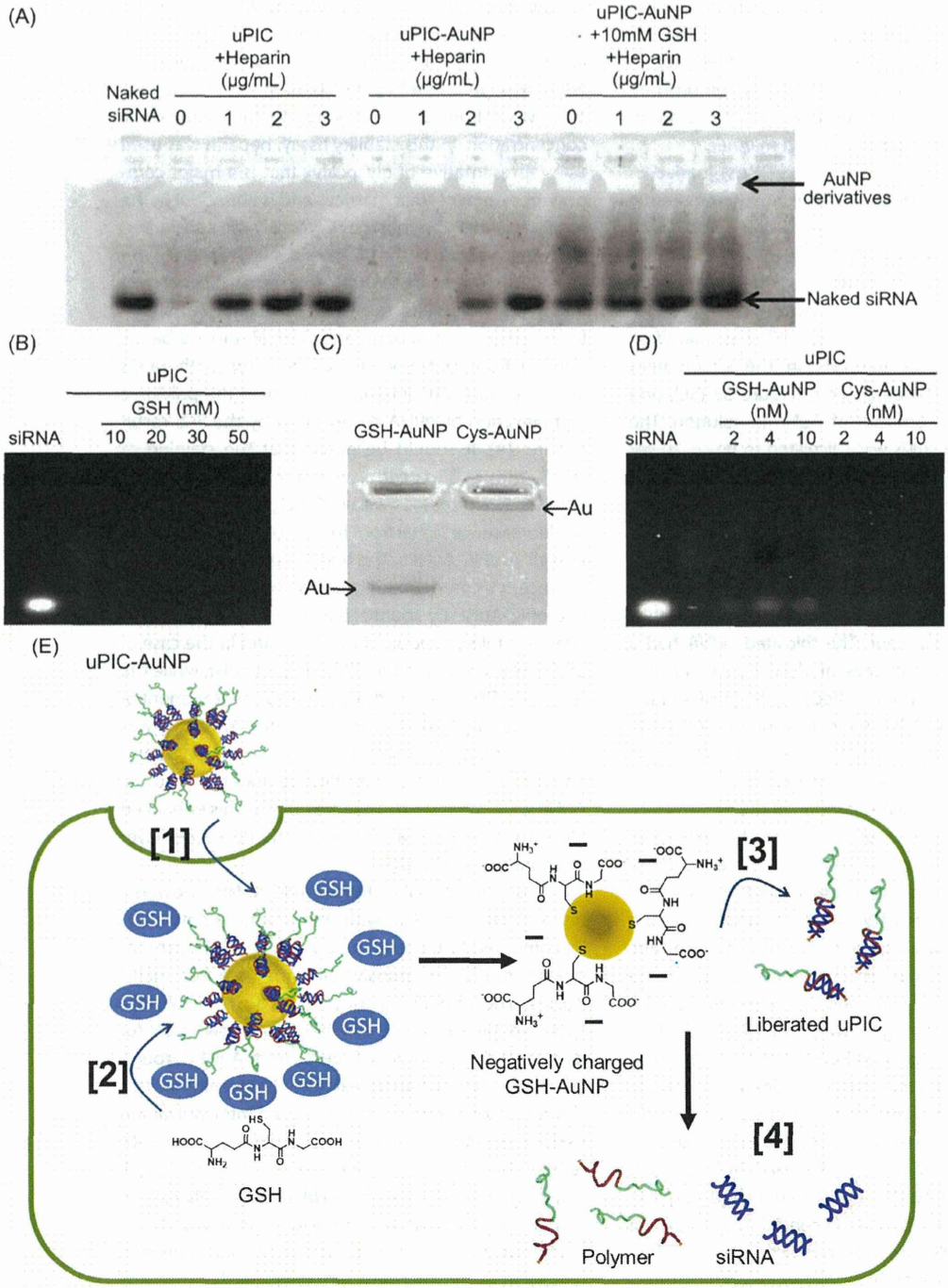

Figure 4. (A) Stability assay of uPICs and uPIC-AuNPs (400 nM siRNA) incubated with heparin (0, 1, 2, and 3 μg/mL) and GSH (0 and 10 mM). At 10 min after incubation, the solutions were loaded onto 1% agarose gel (1 × Tris/Borate/EDTA (TBE) buffer), subjected to a voltage of 100 V for 15 min, and stained with SYBR Green II. (B) Gel electrophoresis of uPICs solutions in the presence of various GSH concentrations. (C) Gel electrophoresis of AuNPs solutions treated with GSH or cysteine. Arrows indicate the AuNP positions. (D) Gel electrophoresis of uPICs solutions in the presence of AuNPs pretreated with GSH (GSH-AuNP) or with cysteine (Cys-AuNP). (E) Schematic illustration of the proposed mechanism for intracellular siRNA release from uPIC-AuNPs in the presence of GSH.

uPICs; the GSH-AuNPs that have negative surface charges derived from one excess of carboxyl group in GSH can bind to oppositely charged PEG-PLL in uPICs, directed toward siRNA release. To verify this assumption, an additional release assay was performed using GSH-AuNPs prepared as a negatively charged nanoparticle and cysteine-conjugated AuNPs (Cys-AuNPs) which were prepared as a control nanoparticle